IT/P1-29

Modelling of Edge Control by Ergodic Fields in DIII-D, JET and ITER.

M. Bécoulet[1], E. Nardon[1],G. Huysmans[1], P. Thomas[1], M. Lipa[1], W. Zwingmann[1], O. Czarny[1], G.Agarici[1], A.Saille[1], J.-M. Verger[1], R.Moyer[2], T. Evans[3], V. Chuyanov[4],G. Federici[4], Y. Gribov[5] , A. Polevoi[5], G. Saibene[6], G. Vayakis[6], A. Portone[6], A. Loarte[6], V. Parail[7], J. Hastie[7], C. Gimblett[7].

[1]Association Euratom-CEA, CEA Cadarache, F-13108, St. Paul-lez-Durance, France
[2]University of California, San Diego, La Jolla, CA 92093, USA
[3]General Atomics, P.O. Box 85608, San Diego, CA 92186-5688, USA
[4]ITER JWS Garching Co-center, Boltzmannstrasse2, 85748 Garching, Germany
[5]ITER Naka JWS, 801-1 Mukouyama, Naka-shi,Ibaraki-ken, 311-0193 Japan
[6] EFDA close Support Unit,2 Boltzmannstrasse,D-85748 Garching,Germany
[7]Euratom/UKAEA Fusion Association, Culham Science Centre, Abingdon,OX143DB, U.K.
e-mail of the main author: marina.becoulet@cea.fr

Abstract. The present paper analyses possibilities of constructing coils systems in ITER and JET that are able to produce Resonant Magnetic Perturbation (RMP) spectra and edge ergodisation similar to the realistic experimental case of the total Type I ELMs suppression at high confinement in DIII-D. Due to the strong technical restrictions for the in-vessel implantation both in JET and ITER, external coil designs were considered initially. However, the large distance from the coils to plasma edge and rapid decay of the magnetic perturbation require much larger currents in ITER *(~600kA)* and JET *(~400kA)* compared to DIII-D *(~3kA)* for typical H-mode scenarios at q_{95}~ 3 and toroidal symmetry $n=3$. Moreover, the coils currents and central perturbations are almost prohibitively large for higher $q_{95}>4$ scenarios. In-vessel coils closer to the plasma mounted on the blanket modules can be optimized for all ITER reference scenarios ($q_{95}=3 \div 5$) at *~25kA*.
The non-linear MHD modelling of the self-consistent plasma response demonstrated plasma density transport due to $\vec{E} \times \vec{B}$ drift generated in the presence of RMPs. The estimations of the screening of RMPs due to toroidal plasma rotation showed a strong decrease of the perturbation amplitude in the plasma centre in DIII-D, JET and ITER, but relatively weak effect in pedestal region depending on the plasma parameters.

1.Introduction.

The reduction of the heat and particles loads on the Plasma Facing Components (PFCs) due to Type I Edge Localized Modes (ELMs) remains a significant research problem for the international tokamak program [1]. Among the possible approaches of ELM control is the idea to use of external perturbing coils to ergodise the edge magnetic field [2,3]. The "radial" magnetic field component, i.e. the perpendicular to the equilibrium magnetic surface, plays the most essential role in the generation of magnetic islands on the rational surfaces $q=m/n$. Here m,n are respectively poloidal and toroidal numbers of the radial magnetic perturbation harmonic's amplitude in flux coordinates [4]. The overlapping of neighboring islands chains is commonly quantified by the Chirikov parameter [4-5], i.e. the ratio of radial islands widths to the radial distance between successive islands chains. For values of the Chirikov parameter >1, the chaotic behavior leading to the effective field lines diffusion (as they travel around the torus) occurs [4]. In this so-called stochastic (or ergodic) region usually an increase of thermal and particle losses is observed [5-6]. The idea to use edge ergodisation for ELMs control [2-3] is based on increasing the edge transport trough the External Transport Barrier (ETB) enough to prevent the pressure gradient from reaching the critical value that triggers ideal MHD instabilities responsible for Type I ELMs [7], thereby suppressing them, while at the same time minimizing a loss of plasma confinement. The

ergodisation in H-mode plasmas can be rather efficient since in the region of ETB the turbulent transport is already reduced to the small neoclassical value (*~0.1m²/s*) and hence even a small increase of the edge transport by a weak ergodisation could be enough for Type I ELMs suppression. A second advantage of the H-mode operation is the strong edge magnetic shear in X-point configurations that eases the overlapping of the islands at the edge since the resonant surfaces are very close to each other. Since the shear decreases very rapidly when one goes towards the plasma center, the islands overlapping gets much less probable in the core. A Resonant Magnetic Perturbation (RMP) generated by I-coils in DIII-D experiments has been proven to be able to suppress the Type I ELMs reliably without significant degradation of plasma confinement [3,8,9-10]. The suppression of Type I ELMs has been obtained in a wide range of plasma configurations and parameters, proving the robustness of these results. The most surprising effect of RMPs in the case of total ELMs suppression at low pedestal collisionality was an increased particle transport manifested in the decrease in the pedestal density, while the electron temperature remained the same and the ion temperature even increases [9,10]. The total pressure gradient decreases gradually with increase in the I-coils current. The MHD stability analysis [10] showed that the pressure gradient and edge current density with RMPs remain within a domain where plasma is stable for the peeling-ballooning modes. From the quasi-linear theory [4-5] for heat and particle diffusion it is difficult to explain DIII-D experimental results. In particular the mechanism of the increased heat transport in the ergodic zone [5], is the appearance of a radial component of the heat flux parallel to the field lines which produces a net radial heat transport with effective heat conductivity in low collisionality plasmas: $\chi_{erg}^{Te} \approx v_{Te} D_{FL}$, where $D_{FL} \sim \pi R q \sum_{resonant\ m,n} (\delta b_{mn})^2$ -is a coefficient of magnetic line diffusion [5]. According to this the predicted heat diffusion coefficient in DIII-D experiments would be unrealistically large for the pedestal region: *~10m²/s* [14]. On the other hand the particle transport in ergodic region (however without drift effects) was predicted to be less efficient because of the obvious ratio between electron and ion thermal velocity $v_{Ti} << v_{Te}$. However the possibility of large induced convective particle transport in ergodic zone due to the electric $\vec{E} \times \vec{B}$ drift was already mentioned in [5]. The present paper summarises the RMPs coils design work that has been done for JET and ITER with the aim to reproduce the level of pedestal ergodisation similar to the DIII-D experimental case. In this modelling the RMPs spectrum was estimated for vacuum fields without plasma effects. On the other hand some essential features of self-consistent plasma response on RMPs are also discussed. In particular the induced plasma density convective $\vec{E} \times \vec{B}$ drift transport was modeled for DIII-D using a non-linear MHD code JOREK [11]. The possible screening of RMPs in DIII-D, JET and ITER due to the toroidal plasma rotation [13,14] is estimated using both analytical and numerical results from JOREK code.

2. RMP spectrum modelling.

The main numerical tools developed to model RMPs spectrums for different machines were presented in [12,15,16]. In this section we give a short summary of the methods. The RMPs coils are represented schematically by zero-thickness wires in 3D space. Assuming the plasma magnetic response to be very small, the perturbation magnetic field is calculated as if in vacuum using Biot and Savart formula in cylindrical coordinates *(R,ϕ,Z)*. A poloidal spectrum of the radial magnetic perturbation is calculated in the intrinsic flux coordinates:

(s,θ,ϕ). Here $s=\sqrt{\psi}\in[0,1]$ is a normalized radial coordinate, ψ is the normalised poloidal magnetic flux, ϕ is the toroidal angle and the poloidal angle θ is defined such that $\frac{d\phi}{d\theta}=-q(\psi)$ -a safety factor. The magnetic equilibrium is calculated using the HELENA code [17]. The perpendicular to the magnetic surface ("radial") component can be represented as $B^{(1)}\approx(\vec{B}_{eq},\vec{\nabla}s)$, where $\vec{B}_{eq}=\vec{\nabla}\phi\times\vec{\nabla}\psi+F\vec{\nabla}\phi$ and $F(\psi)=RB^{\phi}$ is the product of the major radius R and the toroidal magnetic field B^{ϕ}. Notice, that in the equilibrium case without RMPs $B_{eq}^{(1)}=0$. In order to obtain a physical normalized radial component one should use the formula: $b^{(ph)}=(\vec{B}_{eq},\vec{\nabla}s)/(B_{eq}\sqrt{g^{11}})$, where $g^{11}\equiv(\vec{\nabla}s,\vec{\nabla}s)$. The radial component can be presented as a sum over poloidal and toroidal harmonics: $B^{(1)}(s,\theta,\phi)=\sum_{n=-\infty}^{\infty}\sum_{m=-\infty}^{\infty}B_{mn}^{(1)}(s)e^{i(m\theta+n\phi)}$. To estimate the island size and the degree of overlapping of the edge islands and hence the edge ergodisation, Poincaré plots were obtained by integrating the field-line equations [16]. However for a quantitative and more rapid estimation of the level of ergodicity the cylindrical approximation for island width and Chirikov parameter has proven to be rather efficient since its results are very close to direct field-lines integration [16]. Introducing the effective radial coordinate $r=as$ (where a is the minor radius) as a mark for the magnetic surfaces, defining the effective radial coordinate vector as: $\vec{e}_r=\vec{\nabla}s/<g^{11}>_{\theta}$ and using the procedure of field lines integration near resonant surface similar to [18] one obtains the expression for the magnetic island half-width: $\delta_{m,n}\approx\left(4R_0aq^2b_{res}^r/(m\frac{dq}{ds})\right)^{1/2}$, and the distance between the neighbouring surfaces as: $\Delta_{m,m+1}\approx a/(n\frac{dq}{ds})$. The Chirikov parameter $\sigma_{Chir}=(\delta_{m,n}+\delta_{m+1,n})/\Delta_{m,m+1}$ is a characteristic of the degree of overlapping for islands. Here the amplitude of the effective radial perturbation normalised to the magnetic field on the axis is calculated as : $b_{res}^r\sim\left|2B_{mn}^1\right|/(B_0<g^{11}>_{\theta})$ Note that at fixed b_{res}^r and for a given q profile, σ_{Chir} scales as $(R_0a)^{1/2}/a\sim\varepsilon^{-1/2}$ Since ε changes little between DIII-D , JET and ITER , it is equivalent to compare the RMPs strengths between different machines both in terms of Chirikov parameter or in terms of normalized radial magnetic perturbation, provided the q profiles and toroidal n symmetry are similar. Thereby the level of radial magnetic perturbation in DIII-D $b_{res}^r(r=a)\sim2.5\cdot10^{-4}$ obtained from perturbation spectrum modelling for DIII-D experiments

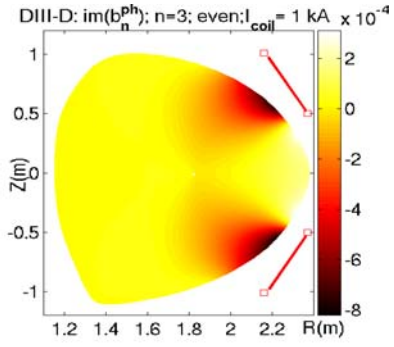

Fig.1. Structure of radial magnetic perturbation in DIII-D. Positions of upper and lower I-coils are indicated by red lines.

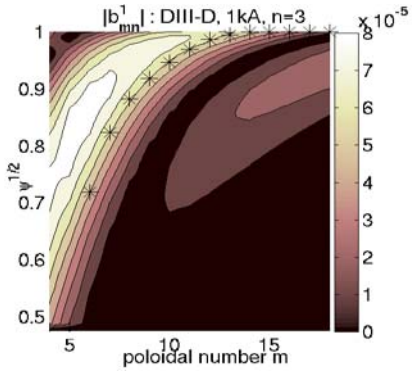

Fig.2. Normalized poloidal spectrum for DIII-D I-coils (even parity) versus radial coordinate and poloidal number for shot DIII-D #115467, q_{95}=3.6. Resonant surfaces q=m/3 are marked by stars.

[16] was taken as a reference for future design modelling for other machines. A poloidal structure (Fig.1) and a poloidal spectrum (Fig.2) of RMPs in the DIII-D experimental case, with I-coils in even parity used as a reference, are presented. The aim of the design work for ITER and JET is to propose the coils system and phasing between coils in a way that edge resonant surfaces $q=-m/n$ (signs of m and n are conventional, but opposite since $q>0$) are situated near the maximum of the spectrum which is the case on Fig.2 for DIII-D. However, notice that the RMPs spectrum is specific for each equilibrium and in particular q-profile through the pitch angles of the field lines as they pass in front of the RMP coils.

3. Modelling of external RMP coils for ITER and JET.

Because of the rapid decrease of the magnetic perturbation with the distance from the coils the RMP coils should be as close as possible to plasma. At the same time the RMP coils should have the possibility of adaptation to different equilibria and q-profiles by phasing between coils in order to generate an optimal spectrum. However, due to the strong technical restrictions for the in-vessel implantation both in JET and ITER, external coil designs were considered initially as the more feasible option. One of the proposed designs for ITER (6 upper and 6 lower coils) and JET (18 upper and 18 lower coils) are presented in Fig.3-4. After studies of the available space in both machines the realistic geometrical parameters are taken into account in these designs compared to the initial work [16]. The $n=3$ toroidal symmetry was taken for both designs [12,16]. The structure of the radial magnetic

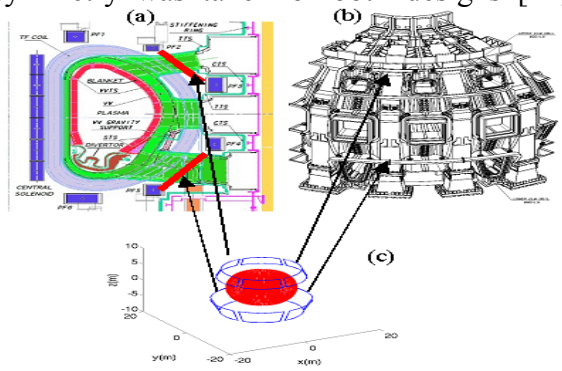

Fig.3 External RMP coils for ITER.

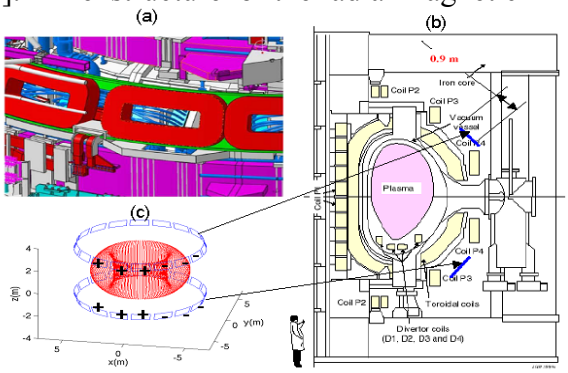

Fig.4 External RMP coils for JET.

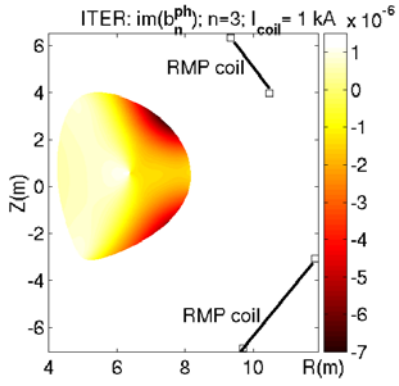

Fig.5. Structure of radial magnetic perturbation in ITER for external coils.

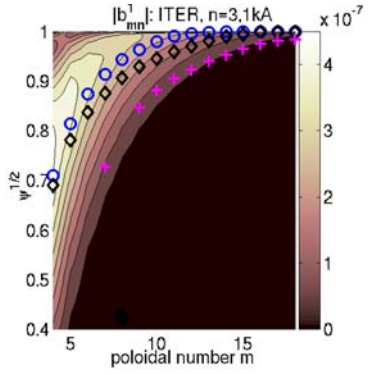

Fig.6.Poloidal spectrum for external coils in ITER. Position of rational surfaces for ITER scenarios [19]: H-mode :q_{95}~3('o') ,Hybrid q_{95}~4('◊'), ITB: q_{95}~5.3('+')

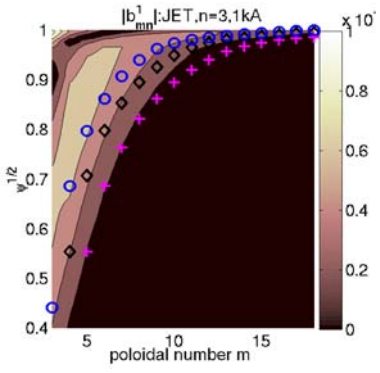

Fig.7.Poloidal spectrum for external coils in JET. Position of rational surfaces for different q profiles: H-mode :q_{95}~3('o'),Hybrid q_{95}~4('◊'), ITB: q_{95}~5.3('+').

perturbation generated by external coils is similar for JET, ITER (Fig.5) and DIII-D (Fig.1). However, because of the larger distance from the RMP coils the amplitude of the high *m* harmonics decreases drastically for corresponding spectra for ITER and JET (Fig.6,7). From the position of the rational surfaces on the spectra in *q* scans one can see that RMPs coils can be reasonably used only in H-mode scenarios [19] with q_{95}~3 $(=m_{res}/3)$. Higher q_{95}=4-5 scenarios are far from the maximum of the resonant harmonics amplitude of the poloidal spectrum both for ITER and JET. The estimations of the averaged radial perturbation (Fig.8,9) and Chirikov parameter (Fig.10) are presented for JET and ITER in comparison with the DIII-D experimental ELMs suppression case at I_{coil}=3kA. Notice that here B_0=5.3T for ITER, B_0=2.7T for JET and 1.6T for DIII-D. One needs ~400kA in JET and ~600kA in ITER for these designs for q_{95}~3 scenarios to reach the same level of edge ergodisation.

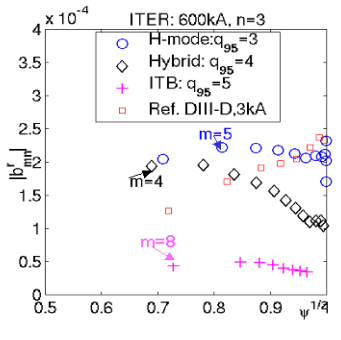

Fig.8. Normalised to the equilibrium field (B_0=5.3T) radial magnetic perturbation generated by ITER external coils at 600kA compared to DIII-D reference case (q_{95}=3.6,B_0=1.6T,Icoil=3kA)

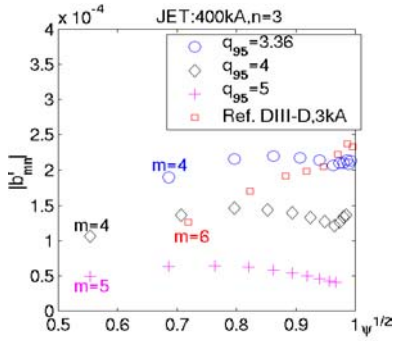

Fig.9. Normalised to the equilibrium field (B_0=2.7T) radial magnetic perturbation generated by JET external coils at 400kA compared to DIII-D reference case.

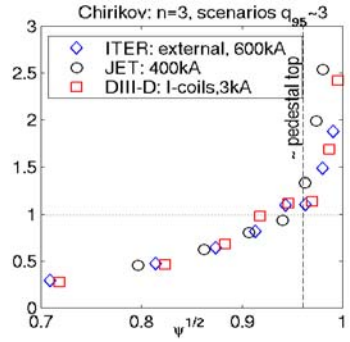

Fig.10.Radial profile of Chirikov parameter for H-mode scenarios at q_{95}~3 for external RMP coils in ITER at 600kA, in JET at 400A compared to DIII-D reference case (I-coils at 3kA,even parity).

4. In-vessel coils for ITER.

We are conscious that in-vessel coils in ITER represent much more technological difficulties in terms of accessibility, cooling, electric connections and insulation of such coils in a reactor environment compared to external coils. However, for in-vessel coils mounted on

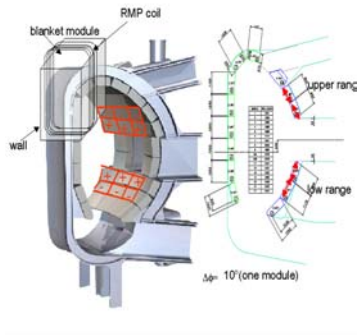

Fig.11. ITER blanket coils. Signs(+ and -) indicate possibility of different current phasing.

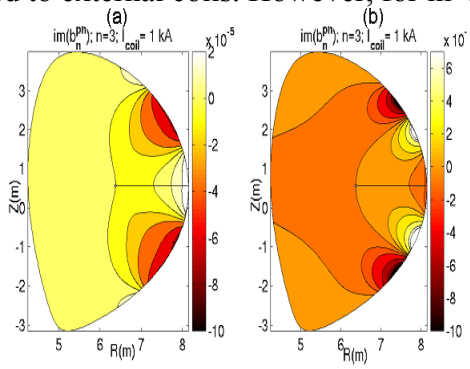

Fig.12. n=3 harmonic amplitude of the radial magnetic perturbation generated by ITER blanket coils with poloidal phasing '++++'(a) and '+--+'(b)

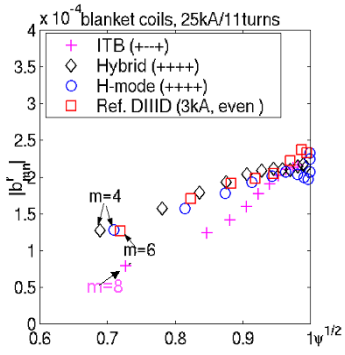

Fig.13.Averaged resonant harmonics amplitude profiles for blanket coils at 25kA/11 turns for ITER

blanket modules (Fig.11) the current can be significantly reduced. Moreover the possible different phasing between modules (i.e. RMP coils) gives a large possibility to adapt a

spectrum to different scenarios. Since each module represent ~*10°* in toroidal direction, to produce *n=3* symmetry one can use 6 upper and 6 lower 'global' coils formed by (5 up +5 down) modules separated toroidally by one module. In the modelling a single coil is represented by 11 turns of wires around each module starting from *6cm* from the surface facing plasma and dispatched over a width *27 cm* towards the wall. The poloidal structure of the magnetic perturbation at different poloidal phasing between coils is presented in Fig.12. The radial perturbation can now be adapted to all ITER reference scenarios (Fig.13): '++++' phasing in poloidal direction (see Fig.11) can be used for H-mode (q_{95}=*3.12*) and Hybrid (q_{95}=*4.12*) scenarios and '+--+' is optimum for ITB scenario (q_{95}=*5.33*).

5. Non-linear MHD modelling of plasma response on RMPs.

In the modelling results described above, the magnetic perturbation is computed in vacuum, neglecting the magnetic plasma response, which could be important. The non-linear MHD modelling in X-point geometry were performed with the code JOREK [11] for RMPs generated by the I-coils in DIII-D (Fig.14). Self-consistent evolution of magnetic flux, vorticity, density and currents generated in plasma were taken into account. Convective plasma density transport due to the $\vec{E} \times \vec{B}$ drift generated in the presence of RMPs was

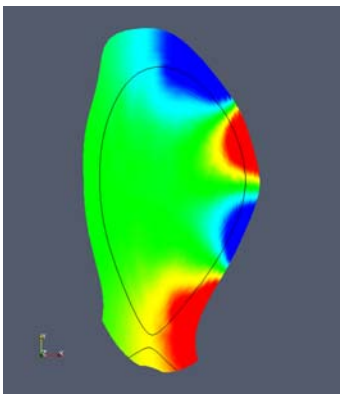

Fig.14. Poloidal magnetic flux perturbation (harmonic n=3) due to I-coils in DIII-D (#122336, I_{coil}=4kA) calculated by code JOREK.

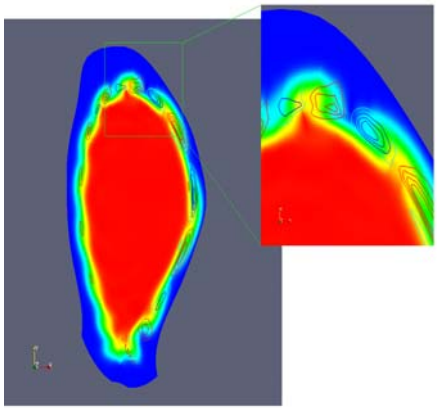

Fig.15. Density map for DIII-D (#122336, Icoil=4kA) after t=10^4 τ_A. Convective cells transport particles to the SOL. Contours represent constant electric potential .

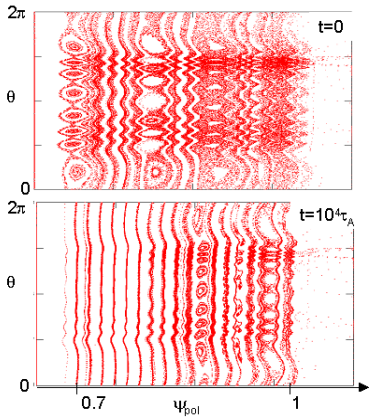

Fig.16.Poincare plots done by code JOREK for DIII-D (#122336, Icoil=4kA) without plasma rotation (upper plot) and with plasma rotation frequency f=2.710^{-3} τ_A^{-1} (down plot).

observed in modelling (Fig.15). In present simulations the initial flat density profile relaxes mainly due to the convection. Here the characteristic time for convective cells formation is ~10^2 τ_A. In present modelling we were interested mainly in description of the convective mechanism of fast density transport through the separatrix, hence particle sources and parallel losses in SOL were not taken into account. Also particle diffusion is much slower process (τ_{diff} ~2.10^5 τ_A). This convective loss can be a candidate to explain density decrease with RMPs in DIII-D [9,10]. However, the convective cells width decreases with decrease of plasma resistivity in the present modelling, hence the efficiency of this mechanism at low collisionality needs more investigations. The RMPs can be amplified by plasma if the edge current density is close to the MHD stability limit for external kink/tearing modes. This effect is in particular more important for a large bootstrap current fraction. On the other hand

the RMPs can be screened by plasma rotation [13,14]. The toroidally rotating boundary condition for magnetic flux perturbation $\delta\psi = \psi_{n=3}\sin(n(\varphi + 2\pi f \cdot t))$ was applied to mimic this effect in the JOREK code since the toroidal momentum is not treated self-consistently in the present version. The Poincare plots with and without plasma rotation are presented on Fig.16. Here $f = 2.7\cdot10^{-3}\ \tau_A^{-1}$ is the plasma toroidal rotation frequency which is considered constant. One can see that island size is significantly reduced especially towards the plasma centre.

6.Analytical estimations of the effect of plasma rotation on RMPs in ITER, JET and DIII-D.

It was shown in the papers [13,14] that if visco-resistive linear layer theory is applicable, the radial component of the vacuum magnetic field in cylindrical approximation on the resonance surface $q=-m/n$ is shielded by plasma rotation: $B_{m,n}^{r,pl} = \dfrac{B_{m,n}^{r,vac}}{\sqrt{1+(\Omega\tau_L/2m)^2}} = S_{fac}B_{m,n}^{r,vac}$. Here $\Omega = 2\pi n f$ is local toroidal rotation frequency for the mode n, τ_L is the visco-resistive layer time: $\tau_L = 2(\sqrt{1+2q^2}\tau_A)^{2/3}\tau_\eta^{2/3}/\tau_v^{1/3}$, $\tau_A = R/V_A\cdot 1/(n\cdot Sh)$ is the Alfvén time, $Sh = r/q(dq/dr)$ is the local magnetic shear, $\tau_\eta = \mu_0 r^2/\eta$ is the resistive time , $r = a\psi^{1/2}$ is an equivalent radius of the resonant magnetic surface in cylindrical approximation, η is the parallel plasma resistivity, $\tau_v = r^2\rho/\mu$ the viscous time (here we take $\mu/\rho \sim 1 m^2/s$). Typical H-mode plasma parameters are used for the estimations in ITER[19], JET [20] and DIII-D[10] are presented in Fig.17.

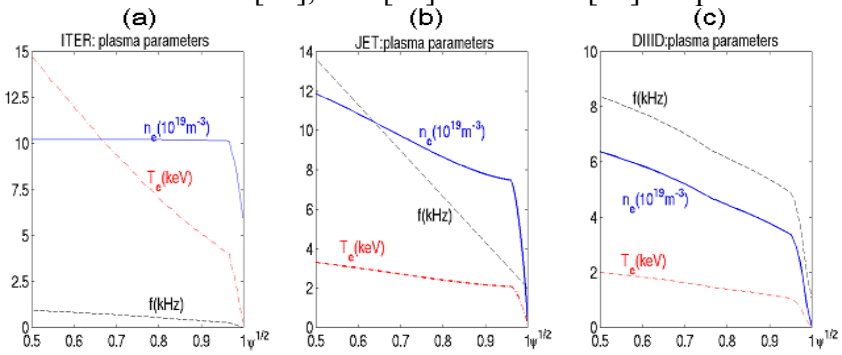

Fig.17. Plasma parameters used for the estimations of screening factor in (a)-ITER, (b)-JET,(c)-DIII-D.

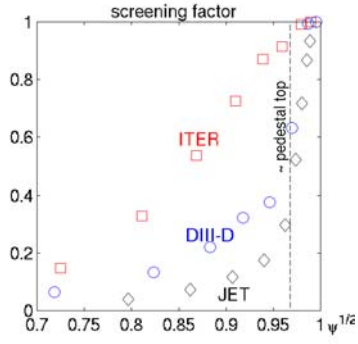

Fig.18. Screening factor S_{fac} for parameters of Fig.17.

The corresponding screening factor S_{fac} is presented on Fig.18. One can see that the screening due to the rotation is most efficient towards plasma centre for all machines (however smaller for ITER because of the slower rotation). The shielding is much smaller in the pedestal due to the slower rotation and also smaller resistive time at the edge compared to the centre. Notice that this analytical estimations for JOREK modelling (Fig.16), where $\tau_\eta/\tau_{A0} \sim 2.10^4, \tau_V/\tau_{A0} \sim 2.10^5, \tau_{A0} = R/V_A$, $n=3$, $m=4$, $Sh\sim0.1$, give $S_{fac}\sim0.7$. The screening on RMPs due to the rotation observed in the modelling (Fig.16) is larger than analytical estimations, suggesting that non-linear and toroidal effects could be important. The analytical estimations presented here should be considered only as an approximate trend, since here the toroidal momentum is not treated self-consistently with plasma response. For example it is known from experiment [10] that static RMPs usually cause more or less important central

plasma braking leading to the decrease of the screening effect and, as a consequence, the RMP field will penetrate more.

7. Conclusions.

Similar ergodisation of the pedestal region (Chirikov parameter ~1 on the pedestal top) is produced by the proposed external RMP coils systems with currents in the coils: *~600kA* in ITER, *~400kA* in JET and by in-vessel I-coils at *3kA* in DIII-D in typical H-mode scenarios at q_{95}~ 3 and toroidal symmetry $n=3$. However due to the drastic decrease of the higher resonant $(q=-m/n)$ poloidal harmonics amplitudes in the RMP spectrum, currents in external RMP coils situated far from plasma and generated perturbations in the plasma centre are prohibitively large for higher $q_{95}>4$ scenarios (Hybrid and ITB). On the contrary, the in-vessel coils mounted on the blanket modules can be optimized for all ITER reference scenarios ($q_{95}=3\div5$) at much lower current *~25kA*. However in-vessel coils design represents many technological difficulties. The possible compromise between external and in-vessel coil designs is still under investigation , but for the moment it is out of the scope of this paper.

The non-linear MHD modelling of the self-consistent plasma response demonstrated convective particle transport due to $\vec{E}\times\vec{B}$ drift generated in the presence of RMPs. The estimations of the screening of RMPs due to the toroidal plasma rotation showed a strong decrease of the magnetic perturbation amplitude towards the plasma centre in DIII-D, JET and ITER, but relatively weak effect in the pedestal region where the resistive time and the toroidal rotation frequency have usually much smaller values compared to the plasma centre. This effect can play a positive role in the suppression of the parasitic central islands generated by RMP coils in order to avoid triggering MHD instabilities in the plasma centre.

This work, supported by the European Communities under the contract of Association between EURATOM and CEA, was carried out within the framework of the European Fusion Development Agreement. The views and opinions expressed herein do not necessarily reflect those of the European Commission.

[1] A Loarte et al. Plasma Phys Control Fus **45** (2003) 1549
[2] A. Grosman et al., J. Nuc. Mater., **313-316** (2003) 1314
[3] T.E. Evans et al., Phys. Rev. Lett. **92** (2004)
[4] A. Samain et al., Phys. Fluids **B5** (1993) 471
[5] P. Ghendrih et al., Plasma Phys. Control. Fusion, **38** (1996) 1653
[6] M. Lehnen et al., J. Nucl. Mater. **337-339** (2005) 171
[7] M. Bécoulet et al., Contribution to Plasma Physics **40** (2000) 251-255
[8] R Moyer et al Phys of Plasmas **12**, 05611(2005) and this conference.
[9] K.H. Burrell et al., Plasma Phys. Control. Fusion **47** (2005) B37–B52
[10] T.Osborne et al., Proc. 32nd EPS Conf. Plasma Physics, Tarragona (2005) P4.012
[11] G.Huysmans, Plasma Phys Control Fus **47**(2005)2107
[12] E. Nardon et al, submitted in J. Nuc. Mater (2006)
[13] A. Cole and R. Fitzpatrick, Phys. Plasmas **13** (2006) 032503
[14] V. Parail et al, this conference.
[15] M. Bécoulet et al., Nucl. Fusion **45** (2005)
[16] M. Bécoulet, et al., Proc. 32nd EPS Conf. Plasma Physics, Tarragona (2005) P2.005
[17] G. Huysmans et al, 1991 Proc. CP90 Conf. on Comp. Phys. Proc. (Singapore: World Scientific) 371
[18] J. Wesson, Tokamaks, Clarendon Press-Oxford, 2004
[19] A. Polevoi et al. in J. Plasma Fusion Res., SERIES, Vol. 5 (2002) 82–87
[20] K.-D. Zastrow et al Nucl. Fusion, Vol. 38, No. 2 (1998)